A Model for Chemical Vapor Copolymerization of *p*-Xylylenes with Vinylic Comonomers: Order of Initiation and Reactivity Ratios

Justin F. Gaynor, Seshu B. Desu,* and J. J. Senkevich

Department of Materials Science and Engineering, Virginia Polytechnic Institute and State University, Blacksburg, Virginia 24061-0237

Received January 11, 1995; Revised Manuscript Received July 3, 1995[⊗]

ABSTRACT: A model for chemical vapor homo- and copolymerization is presented in two dimensions, allowing determination of order of initiation in homopolymers and reactivity ratios in copolymers. The model assumes a linear pressure gradient along the flow direction and allows calculation of the order of initiation if thickness vs position are known, and r_1 and r_2 if the gas flow rates, final film thickness, and film composition vs distance are known. Experiments indicate the number, Λ, of *p*-xylylene molecules required to initiate polymerization: For poly(*p*-xylylene) and poly(*p*-chloroxylylene), $\Lambda = 3$; for poly(*p*-dichloroxylylene), $\Lambda = 4$. Tentative values for the reactivity ratios of poly(*p*-chloroxylylene) with perfluorooctyl methacrylate have been determined at different temperatures. At 20 °C, $r_1 = 13.04$ and $r_2 \approx 0$; r_1 increases with increasing temperature, while r_2 remains vanishingly small.

Introduction

The chemical vapor polymerization (CVP) of poly(*p*-xylylene) (PPX), first reported in 1947,[1] was first modeled by Beach[2] and has been thoroughly reviewed.[3–6] Dicyclo-*p*-xylylene sublimates under vacuum and passes through a hot pipe where it decomposes into two *p*-xylylene (PX) molecules. The monomer then flows into a cooler deposition chamber; though still at a pressure below its vapor pressure, it has a finite residence time on the chamber walls. A small fraction is consumed by either initiation or propagation; the remainders reenter the gas. Spontaneous initiation occurs when a small number (Λ) of PX molecules convert into a single diradical, as shown in Figure 1. Because Λ is greater than 1, polymerization in the gas phase is unlikely; the monomer is present in sufficient concentrations for initiation only after adsorption on the chamber walls. After a stable diradical has formed, both PX and vinylic comonomers can add by free-radical addition.

Recently, several vinylic monomers, including maleic anhydride, 4-vinylbiphenyl, 9-vinylanthracene, and perfluorooctylmethacrylate, have been found to form copolymers when deposited at room temperature, significantly altering the final properties of the film.[7,8] Copolymers of poly(*p*-chloroxylylene) (PPX-C) and perfluorooctylmethacrylate (PFOMA), for example, show lower dielectric constants than PPX-C homopolymers; we have grown copolymers with dielectric constants of 1.92 at optical frequencies, compared to 2.66 for the homopolymer. Other copolymers may show higher thermal stability than PPX-C homopolymers, which degrade above 230 °C.

Here, we extend the model proposed by Beach to two dimensions, allowing calculation of reactivity ratios and determination of the order of initiation. Homopolymers of the three commercially available monomers and a copolymer film of PPX-C and PFOMA will be discussed in the Experimental Section to demonstrate the method.

Order of Initiation. An unanswered question in the PPX literature is the exact order of the initiation reaction, in other words, the exact number of monomers,

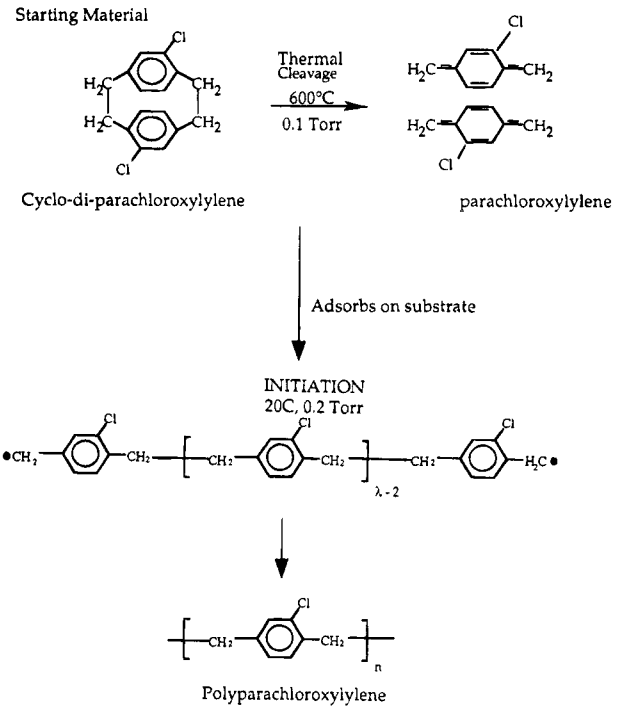

Figure 1. Reaction pathway for initiation and polymerization.

Λ, required to form a stable aromatic diradical from the aliphatic monomers. Beach derived the following equation relating growth rate to monomer partial pressure:[2]

$$\gamma = \left(\frac{2}{\lambda\varrho^3}\right)^{1/4}(k_i k_p D^2)^{1/4}\left(\frac{\varrho}{K_H p_0}\right)^{((\lambda+3)/4)} p^{((\lambda+3)/4)} \quad (1)$$

where γ is the growth rate, p is the monomer pressure, k_i and k_p are the initiation and propagation rate constants, D is the diffusion rate constant of monomer into the film, p_0 is the monomer vapor pressure, and K_H is the Henry constant. Thermodynamic calculations[3] predict $\Lambda = 3$, implying the growth rate increases as $p^{1.5}$. However, a widely cited early paper shows the growth rate increasing as the square of monomer pressure.[9] It is difficult to judge the reliability of these results, though, as neither data points nor error bars were supplied, nor was the experimental method de-

[⊗] Abstract published in *Advance ACS Abstracts,* October 1, 1995.

0024-9297/95/2228-7343$09.00/0

scribed. By considering changes in gas flow direction as well as growth in the radial direction, we are able to suggest a simple method to determine Λ. If we define the direction of gas flow as z, then the growth rate will depend on z as follows:

$$Gt = T; \quad \frac{\partial G}{\partial z} = \frac{\partial T}{\partial P}\frac{\partial P}{\partial z}$$

where G is the growth rate, T is film thickness, t is time, and P is monomer partial pressure. dT/dz is easily measured; we suggest a relation for dP/dz to find the dependence of growth rate on pressure.

Reactivity Ratios. The only information required for the determination of reactivity ratios in solution is the feed composition, f, and final composition, F, along with the precision with which they are measured.[10] (Throughout this paper, we use the convention that f and F refer to the mole fraction of PX.) In CVP, it is difficult, if not impossible, to measure the gas composition at the growth interface. Any model to determine CVP reactivity ratios must sidestep this problem. To do this, we recognize a feature unique to CVP: The two monomers will generally be consumed at different rates as they flow through the reaction vessel, generating a steady-state monomer concentration profile in both the gas and the film. For a given composition profile in the gas, there will result a unique composition profile in the film. We show it is sufficient to determine the film composition and thickness as a function of position to determine reactivity ratios. We also note that, during CVP, in contrast to solution reactions, the reaction continues indefinitely without drift in feed composition at any given point, making the problem time-independent.

All reactivity ratios show a temperature dependence, as they are simply ratios of reaction rate constants. PX polymerization typically occurs near its "ceiling temperature"; this is not the thermodynamic ceiling temperature[11] but rather an arbitrarily assigned temperature above which growth rates are negligible. Under typical deposition conditions, the growth rate will decrease with increasing temperature because the molecules reside for a shorter time on the surface. The reactivity ratios as calculated by the model presented here contain both residence time and reaction rate components and may be expected to show a larger temperature dependence than is found in solution work.

The Model

Introduction. The model is presented in cylindrical coordinates to describe deposition in a cylindrical deposition chamber held at constant, uniform temperature. PX molecules (and, during copolymerization, a vinylic comonomer) are forced through the chamber by a pressure gradient and react on the walls. Polymerization starts upon adsorption and proceeds inward in the negative r direction; the monomer concentrations and growth rate change in the flow direction, z, as monomers are consumed. We assume the comonomer does not affect the initiation reaction, there are no penultimate effects or complex formation, and film growth has no θ dependence.

Order of Initiation. There are two sources of pressure gradients in a PX reactor. The first arises from the pressure difference between the monomer sources and the pump. The second arises from the monomer depletion region immediately above the growth surface, leading to radial diffusion. However, for every molecule added to the film, 10^2–10^3 adsorbed molecules reenter the gas without reacting.[3] The radial pressure gradient is negligible, therefore, and we ignore its contribution to the pressure profile.

Assumption 1: *The pressure gradient is linear within the deposition pipe.* Within the chamber,

$$P_{(z)} = (z_f - z)(P_1 - P_2) \tag{2}$$

where P_1 is the pressure at the chamber entrance, P_2 is the pressure at the downstream end of the pipe, and z_f is the position of the downstream end of the pipe. This assumption allows a simple experiment to determine Λ: By measuring the thickness of a film vs position in the reactor, the data should fit a curve of $T = kz^{((\Lambda+3)/4)} + k'$, where k and k' are empirical constants. If $\Lambda = 3$, G should decrease as $z^{1.5}$. Experiments to determine Λ for each of the three commercially available homopolymers are described in the Experimental Section.

Reactivity Ratios. We begin with the following differential form of the Lewis–Mayo equation:[12]

$$F = \frac{(r_1 - 1)f^2 + f}{(r_1 + r_2 - 2)f^2 + 2(1 - r_2)f + r_2} \tag{3}$$

and its integrated form as written by Meyer and Lowry[13]

$$x = 1 - \left(\frac{f}{f_0}\right)^{\alpha}\left(\frac{1-f}{1-f_0}\right)^{\beta}\left(\frac{f_0 - \delta}{f - \delta}\right)^{\gamma}$$

$$\alpha = \frac{r_2}{1 - r_2}; \quad \beta = \frac{r_1}{1 - r_1}; \quad \delta = \frac{1 - r_2}{2 - r_1 - r_2}; \quad \gamma = \frac{1 - r_1 r_2}{(1 - r_1)(1 - r_2)} \tag{4}$$

Solving eq 3 explicitly for f gives a quadratic equation with two real roots. Only the negative root is physically meaningful, however; the positive root yields a negative value of f. The final expression for $X_{(F)}$ is

$$X_{(F)} = 1 - \left(\frac{\dfrac{(r_1 - 1)F^2 + F}{(r_1 + r_2 - 2)F^2 + 2(1 - r_2)F + r_2}}{f_0}\right)^{\alpha} \times \left(\frac{1 - \dfrac{(r_1 - 1)F^2 + F}{(r_1 + r_2 - 2)F^2 + 2(1 - r_2)F + r_2}}{1 - f_0}\right)^{\beta} \times \left(\frac{f_0 - \delta}{\dfrac{(r_1 - 1)F^2 + F}{(r_1 + r_2 - 2)F^2 + 2(1 - r_2)F + r_2} - \delta}\right)^{\gamma} \tag{5}$$

Recognizing that the monomer consumption in CVP is simply the number of monomers incorporated into the film divided by the number of monomers introduced into the chamber, we derive an expression for $X_{(z)}$:

$$X = \frac{\text{monomer in film}}{\text{monomer entering chamber}} = \frac{VN_A/V_m}{(N_{PX} + N_{co})} \tag{6}$$

where V is the volume of the film, V_m is the molar volume of the film, N_A is Avagadro's number, and N_{PX} and N_{co} represent the number of each monomer entering the chamber in a given period of time.

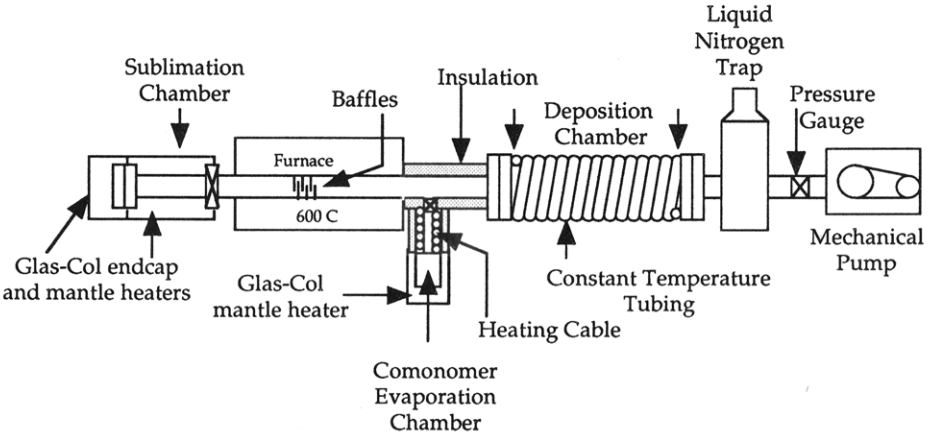

Figure 2. Reaction chamber used for homo- and copolymerization.

Assumption 2: *The relative concentration of monomers at the surface is equal to the relative concentration of monomers in the gas.* This approximation was recognized early in theoretical descriptions of low-pressure chemical vapor deposition (LPCVD) systems. It is valid if the diffusion rates in the gas phase are very high for each monomer and the residence time of each monomer on the surface is the same. Gas-phase diffusion in PX chambers is probably higher than other LPCVD systems, as they operate at lower pressures. Differences in residence times are incorporated into the reactivity ratio, as discussed in the introduction.

Assumption 3: *All reactions occur at the surface.* This assumption allows us to ignore the differing rates of diffusion of each species, including monomers and oligomers, into the film. Beach's model suggests reactions occur throughout the top 400 nm of the film; however, growth is fastest at the surface and decreases rapidly with distance from the interface.

The volume of the film is given by

$$V = \pi R^2 \int \mathrm{d}z - \pi \int (R - T)^2 \,\mathrm{d}z = 2\pi R \int T \,\mathrm{d}z - \pi \int T^2 \,\mathrm{d}z \quad (7)$$

We can ignore the final integral; R is typically 4 or 5 orders of magnitude higher than T. To let thickness increase with increasing z, we define $z = 0$ as the downstream end of the chamber, with z increasing upstream to $z = L$ at the chamber entrance. Combining the above two equations and integrating in the direction of gas flow yields

$$X_{(z)} = \frac{2\pi R N_A}{N_{PX} + N_{co}} \int_L^z \frac{T}{V_m} \,\mathrm{d}z \quad (8)$$

The success of the model depends on equating $X_{(F)}$ and $X_{(z)}$. The molar volume in the integral above is a function of composition; we cannot solve X explicitly as a function of z. Therefore, we employ an average molar volume, $\langle V_m \rangle$, which is not a function of position. This restricts the range of the model's validity to monomers with similar molar volumes or to small ranges of composition. Finally, we assume the film thickness varies as $Az^{1.5} + B$ for PPX and PPX-C, and as $Az^{1.75} + B$ for poly(*p*-dichloroxylylene) (PPX-D); in the Experimental Section, we demonstrate this is indeed the case for homopolymers. Within the model's range of validity, i.e., where the molar volume of the film can be considered independent of position, this is a reasonable assumption. The final expression from which reactivity ratios are determined is

$$\left(\frac{(r_1 - 1)F^2 + F}{\dfrac{(r_1 + r_2 - 2)F^2 + 2(1 - r_2)F = r_2}{f_0}}\right)^{\alpha} \times \left(\frac{1 - \dfrac{(r_1 - 1)F^2 + F}{(r_1 + r_2 - 2)F^2 + 2(1 - r_2)F + r_2}}{1 - f_0}\right)^{\beta} \times \left(\frac{f_0 - \delta}{\dfrac{(r_1 - 1)F^2 + F}{(r_1 + r_2 - 2)F^2 + 2(1 - r_2)F + r_2} - \delta}\right)^{\gamma} = \frac{2\pi R N_A \langle V_m \rangle}{N_{PX} + N_{co}} \left[\left(\frac{AL^{2.5}}{2.5} + BL\right) - \left(\frac{Az^{2.5}}{2.5} + Bz\right) + C\right] \quad (9)$$

The right-hand side of this equation will be referred to as $Z_{(z)}$. This equation has interesting consequences. If $f = (1 - r_2)/(2 - r_1 - r_2)$, or if $r_1 = r_2$, the equation becomes meaningless; these are the azeotropic conditions, when we would expect F to become constant in $Z_{(z)}$.

A curve-fitting procedure is used to determine the reactivity ratios. C, r_1, and r_2 are varied to fit eq 9 to the experimentally determined values of F and $Z_{(z)}$. All sources of error must be considered during curve fitting to obtain reliable values and confidence intervals. When eq 3 is used to determine the reactivity ratios of solutions, for instance, linear least-square fits are invalid[15] because the errors in F and f are approximately equivalent. Computer programs for valid curve-fitting procedures in solution are commercially available; this model requires similar software.[16] As shown in the experimental section, eq 9 properly predicts the shape of F vs $Z_{(z)}$ data. However, in the absence of a statistically valid curve-fitting procedure, our estimates of r_1 and r_2 must be considered tentative at best. More importantly, we are unable to provide intervals of confidence at this time.

Experimental Section

The Reactor. All samples were grown in a cylindrical chamber designed for obtaining a wide range of data. A schematic of the self-built reactor is given in Figure 2. The deposition tube was 35 cm long and 7.62 cm in diameter; temperature uniformity was ensured by wrapping the entire length tightly with 0.25-in. diameter copper tubing connected to the chamber by thermally conductive epoxy. Water pumped

through the copper tubing from a constant-temperature water circulating bath allowed various deposition temperatures. Thermocouples were attached to the outer wall of each chamber to monitor temperature.

Homopolymers. Cyclodi-*p*-xylylene, cyclodi-*p*-chloroxylylene, and cyclodi-*p*-dichloroxylylene, the three commercially available dimers, were purchased from Specialty Coatings and used to grow homopolymers of PPX, PPX-C, and PPX-D. The compounds were used as received but outgassed at 0.28 Torr for 2 h before use. The thickness of the films was kept low because our method of measuring thickness, variable-angle spectroscopic ellipsometry, is more accurate at lower thicknesses. Each homopolymer was grown on a clean, polished silicon strip, 10 cm × 3 cm, placed near the downstream end of the reactor. At the downstream end, deposition rates are low and the monomer is completely cooled. The substrates were blown dry with compressed air before use and handled with gloves at all times. The base pressure during each deposition was 0.275 ± 0.005 Torr.

The cyclodi-*p*-xylylene sublimation temperature was maintained at 138.5 ± 0.5 °C, the thermal cleavage furnace was maintained at 620 °C, and the temperature between the furnace and the deposition chamber was maintained above 60 °C. The temperature of the deposition pipe was 23.2 ± 0.3 °C throughout the deposition. The cyclodi-*p*-chloroxylylene sublimation chamber was maintained at 133.5 ± 0.5 °C; the thermal cleavage furnace was maintained at 620 °C, and the temperature between the furnace and the deposition pipe was maintained above 125 °C. The temperature of the deposition chamber was 26.6 ± 0.4 °C throughout the deposition. The cyclodi-*p*-dichloroxylylene sublimation chamber was maintained at 139.5 ± 0.5 °C, the thermal cleavage furnace was maintained at 620 °C, and the temperature between the furnace and the deposition pipe was maintained above 150 °C. The temperature of the deposition chamber was 38.6 ± 0.2 °C throughout the deposition. Each deposition lasted 60 min.

After growth, each film was annealed for 12–15 h at 106 °C and 0.28 Torr; the temperature was returned to room temperature over a period of 2 h before returning the sample to atmospheric pressure. Annealing was performed to rid the film of unreacted monomer and other impurities, as well as to reduce local variations in density and thickness.

Copolymers of PPX-C and PFOMA. The copolymer films were thicker than the homopolymer films to ensure the electron beam used for elemental analysis would not penetrate the sample, causing erroneous readings. PFOMA (>99%) was purchased from Monomer Polymer. PFOMA and PPX-C were chosen because of the ease with which chlorine and fluorine are resolved in an electron probe and because we predict they form random copolymers. Finally, high growth rates are achieved at relatively high deposition temperatures for PPX-C; high deposition temperature ensured the range of composition would be small. Three runs were performed at deposition temperatures of 20, 24, and 28 °C. Three clean silicon substrates, each 10 cm × 1 cm, were placed end to end in the deposition chamber before each run. In each case, the cyclodi-*p*-chloroxylylene sublimation chamber was maintained at 115 °C, the PFOMA sublimation temperature at 54 °C, and the furnace at 620 °C.

For each run, ~4 grams of cyclo-di-*p*-chloroxylylene and 3 g of PFOMA were weighed into ceramic boats, placed in their appropriate chambers, and a vacuum was immediately pulled. Valves between the sublimation chambers and main reactor were closed after the pressure in the chamber reached its base pressure, which required ~1 min. During this minute, we assume the amount of monomer entering the deposition chamber was negligible because the boats require more than 1 min to reach thermal equilibrium with the sublimation chamber walls. All temperatures were then allowed to stabilize for 20 min before the valves were opened, starting deposition. Deposition times were 60 min at 20 °C, 75 min at 24 °C, and 90 min at 28 °C so that each run would result in similar film thicknesses. The unsublimated cyclo-di-*p*-chloroxylylene and PFOMA were weighed after each deposition to determine the amount of each monomer that entered the chamber. Each sample was annealed as described in the homopolymer section.

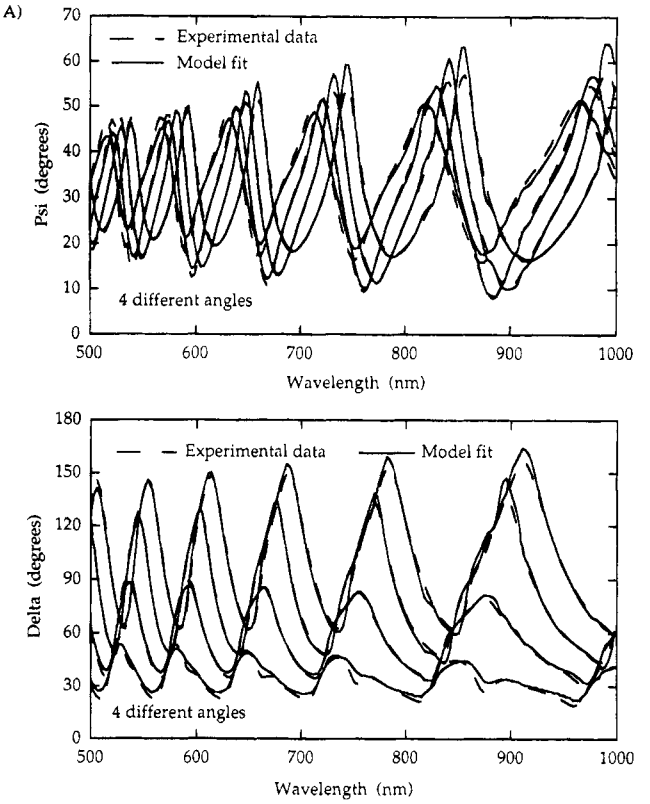

Figure 3. Typical match between variable-angle spectroscopic ellipsometry data and model, yielding film thickness.

Analysis. Absolute elemental compositions were determined by wavelength-dispersive analysis with a Cameca SX-50 electron probe. Electrical conductivity was ensured with a 25-nm-thick sputtered coating of carbon. A 5-nA, 8-kV beam, ~500 nm in diameter, was rastered through an area of 30 μm × 30 μm. Poly(tetrafluoroethylene), poly(chlorotrifluoroethylene), and a PPX-C homopolymer were used as calibration standards. Measurements points were at 1-cm intervals, with three measurements made at each point. The films darkened somewhat during the measurements, each of which lasted 40 s.

Film thicknesses and refractive indexes were determined with a variable-angle spectroscopic ellipsometer, purchased from J. Woollam Co. Samples were measured in the wavelength range 500–1000 nm in 2-nm increments and at angles from 65 to 80° in 5° increments from a line normal to the plane of the film. The homopolymers were measured in 0.5-cm increments, and the copolymers in 1-cm increments. The instrument measures the ellipsometric parameters ψ and δ; each point was the average of 10 measurements. The measurement spot was about 1 mm × 3 mm. For modeling the data, each film was assumed to be birefringent and transparent; the dispersion relations both perpendicular and normal to the film were assumed to fit Cauchy's equation. The birefringent Cauchy model was in excellent agreement with the experimental data; a typical example is shown in Figure 3. The use of variable-angle spectroscopic ellipsometry for measuring CVP films is discussed in more detail elsewhere.[17] The largest systematic error was found to be from placement of the sample in the ellipsometer; for this reason, each homopolymer thickness determination is the average of five measurements, with the sample being removed and replaced between measurements. The largest standard deviation for any sample was 0.41%; typical standard deviations were 0.20%.

The copolymer films were only measured once; the same anisotropic Cauchy model was used for curve fitting. As film thicknesses exceeded ~5 μm, the data became too noisy for reliable thickness determination. Only points with good

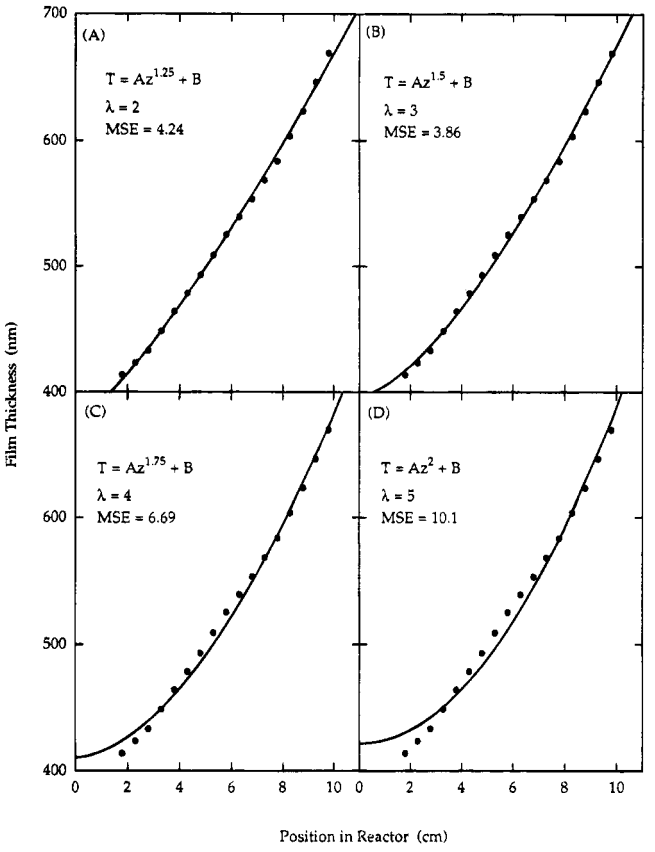

Figure 4. Film thickness vs position in reactor for poly(*p*-xylyene). Each quadrant employs a different curve fit as indicated.

agreement between the model and the experimental data were considered in determining the constants A and B.

Results and Discussion

Order of Initiation. Figures 4–6 show thickness vs position for CVP homopolymers. Error bars are not shown due to extremely small standard deviations (~0.2%) in the measurements. Four different fits are shown for each material as indicated; the values of Λ and the root-mean-square error are presented on each graph. The best fit for PPX, shown in Figure 4, is obtained for $\Lambda = 3$. We conclude polymerization is initiated by three *p*-xylylene molecules combining to form a trimer diradical, in accordance with prediction.[3]

The PPX-C film data also most closely matched the curve obtained from $\Lambda = 3$, as shown in Figure 5. The data for PPX-D, shown in Figure 6, best matched the curve obtained from $\Lambda = 4$. This suggests that four *p*-dichloroxylylene molecules were required to initiate polymerization, forming the tetramer diradical. Recent molecular orbital calculations suggest chlorine acts as a mildly deactivating electron donor in the monomer;[18] perhaps two chlorines sufficiently reduce the polarizability of the monomer that initiation requires four monomers rather than three. The exact role played by substituents during initiation, however, remains to be determined.

Reactivity Ratios. The value for r_1 was found to increase with increasing temperature: 13.04 at 20 °C, 19.07 at 24 °C, and 33.99 at 28 °C. Both r_1 and its temperature dependence are very high in the deposition temperature range studied. This is not surprising; PX is extremely reactive and the deposition temperatures were very close to the PFOMA sublimation temperature,

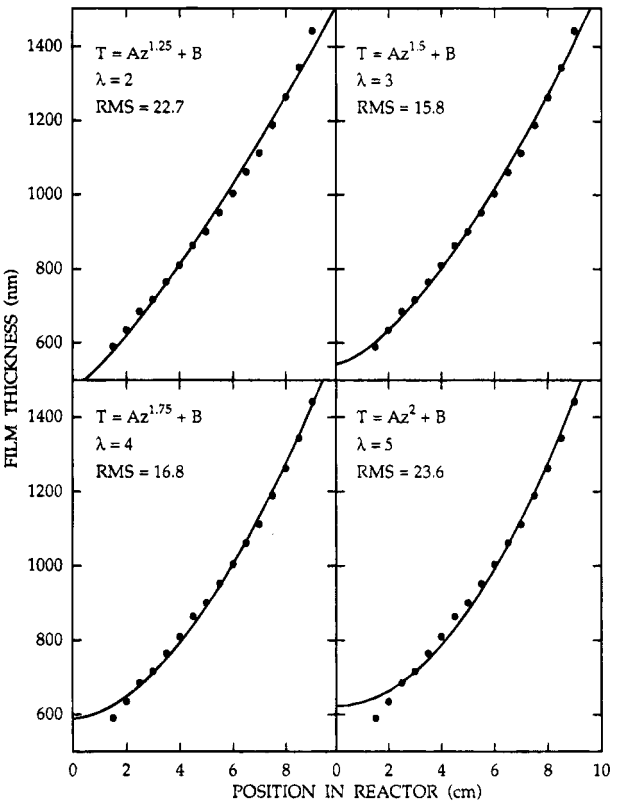

Figure 5. Film thickness vs position in reactor for polychloro-*p*-xylylene. Each quadrant employs a different curve fit as indicated.

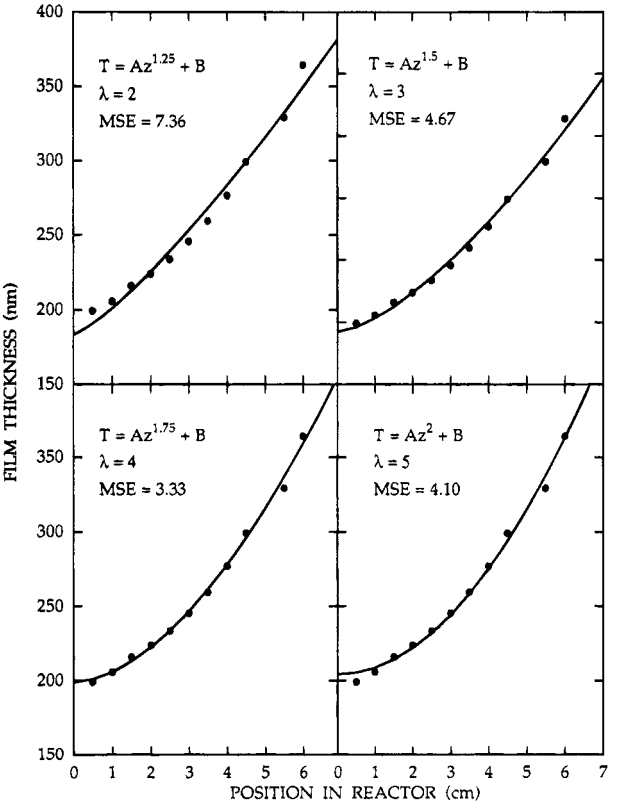

Figure 6. Film thickness vs position in reactor for polydichloro-*p*-xylylene. Each quadrant employs a different curve fit as indicated.

suggesting the residence times on the walls of PFOMA were very short. At each temperature, r_2 was found to be approximately zero (~10^{-8}), though always positive. Figure 7 shows the thickness vs z data from which A

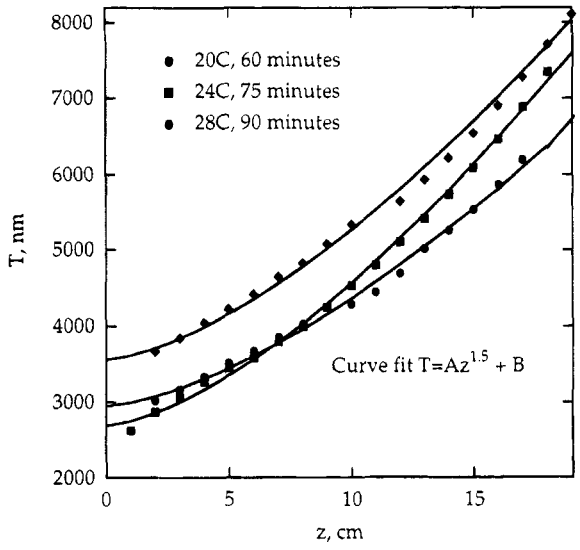

Figure 7. Thickness vs distance for copolymer films, from which $Z_{(z)}$ is calculated.

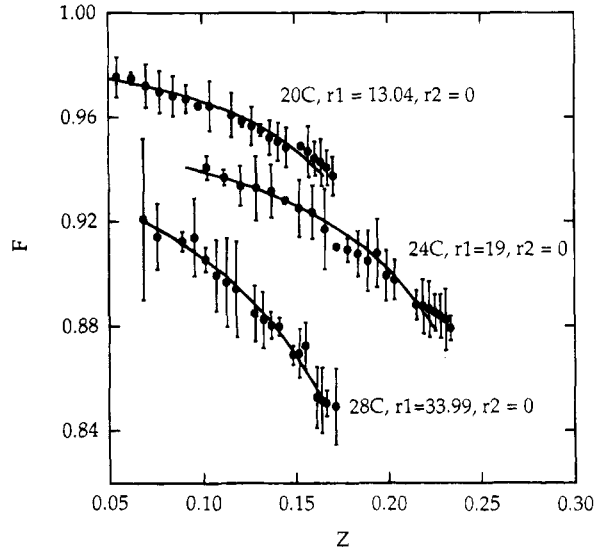

Figure 8. Composition of copolymer films grown at different temperatures vs $Z_{(z)}$, along with curves predicted by eq 9.

and B were calculated for each run. Figure 8 shows each of the three sets of data along with the curve fit obtained from the reactivity ratios listed above.

As discussed earlier, we have not yet developed a statistically valid curve fitting method for obtaining reactivity ratios, nor can we calculate regions of joint confidence. However, we have shown the curve generated by eq 9 provides a satisfactory fit to the experimental data. In addition, the values obtained for r_1 and r_2 are not unreasonable. We note that the precision with which film thickness can be measured is often better than the precision of composition measurements; if the difference in precision is significant, linear least-squares fitting will give acceptable "initial guess" values of the reactivity ratios, though no information about joint confidence regions.[16]

Summary

A model for chemical vapor polymerization in two dimensions is presented which allows determination of the order of initiation and reactivity ratios for random copolymers. We assume that monomer pressure is determined primarily by a linear pressure gradient which forces gas through a cylindrical reaction chamber. This assumption suggests the thickness of a film will vary as $z^{(\Lambda+3)/4}$ if z is the flow direction and Λ is the number of monomers required for spontaneous initiation. Our experimental results suggest that $\Lambda = 3$ for PPX and PPX-C, while $\Lambda = 4$ for PPX-D.

If PPX is grown in the presence of a reactive vinylic comonomer, a copolymer film will result with a composition gradient in the z direction. We equate the monomer conversion as a function of reactivity ratios to the monomer conversion as a function of film volume. This yields an equation that satisfactorily describes experimentally determined composition gradients. The reactivity ratios can be varied to obtain the best fit of composition vs a function of position in the reactor. Until a statistically valid curve-fitting algorithm is developed, reactivity ratios can only be estimated.

Acknowledgment. The authors gratefully acknowledge the assistance of Todd Solberg of the Virginia Tech Department of Geological Sciences for performing the wavelength-dispersive analysis measurements, as well as Dr. Hemanshu Bhatt of the Virginia Tech Department of Materials Science for helpful discussions.

References and Notes

(1) Swarc, M. *Discuss. Faraday Soc.* **1947**, *2*, 46.
(2) Beach, W. F. *Macromolecules* **1978**, *11*, 72.
(3) Beach, W. F.; Lee, C.; Bassett, D.; Austin, T.; Olson, R. *Encyclopedia of Polymer Science*; Wiley and Sons Interscience: New York, 1989; Vol. 17, pp 990–1024.
(4) Beach, W. F.; Austin, T. 2nd International SAMPE Electronics Conference, June 25–35, 1988.
(5) Szwarc, M. *Polym. Eng. Sci.* **1976**, *16* (7), 473–479.
(6) Yasuda, H. K.; Yeh, Y. S.; Fusselman, S. *Pure Appl. Chem.* **1990**, *62* (9), 1689–1698.
(7) Sochilin, V.; Mailyan, K.; Aleksandrova, L.; Nikolaev, A.; Pebalk, A.; Kardash, I. Plenum Publishing document 0012-5008/91/0007-0165, transl. from *Dokl. Akad. Nauk SSSR* **1991**, *319* (1), 173–176.
(8) Gaynor, J. F.; Desu, S. B. *J. Mater. Res.* **1994**, *9* (12), 3125–3130.
(9) Cariou, F. E.; Valley, D. J.; Loeb, W. E. *Proc. IEEE Electron. Pack. Conf.* **1965**, 54–59.
(10) Behnken, G. R. *J. Polym. Sci. A* **1964**, *2*, 645.
(11) Charlson, E. M.; Charlson, E. J.; Sabeti, R. *IEEE Trans. Biomed. Eng.* **1992**, *39* (2), 202–206.
(12) Patino-Leal, H.; Reilly, P. M.; O'Driscoll, K. F. *J. Polym. Sci.: Polym. Lett.* **1980**, *18*, 219–227.
(13) Meyer, V. E.; Lowry, G. C. *Polym. Sci. A* **1965**, *3*, 369.
(14) Gorham, W. F. *J. Polym. Sci., A-1* **1966**, *4*, 3027.
(15) Tidwell, P. W.; Mortimer, G. A. *J. Macromol. Sci.—Rev. Macromol. Chem.* **1970**, *C4*, 281.
(16) Dubé, M.; Sanayei, A.; Penlidis, A.; O'Driscoll, K. F.; Reilly, P. M. *J. Polym. Sci. A: Polym. Chem.* **1991**, *29*, 703–708.
(17) Gaynor, J. F.; Desu, S. B., submitted for publication to *J. Mat. Res.*
(18) Alexandrova, L.; Salcedo, R. *Polymer* **1994**, *35* (21), 4656–4658.

MA950027G